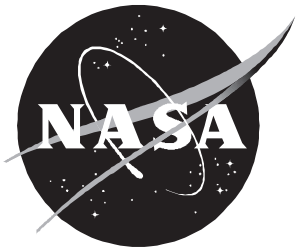

NASA Technical Memorandum 4559

Oxidation Performance of Platinum-Clad Mo-47Re Alloy

Ronald K. Clark and Terryl A. Wallace

June 1994

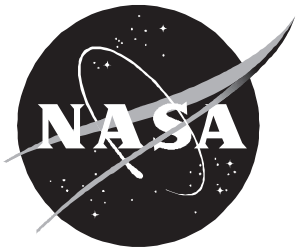

NASA Technical Memorandum 4559

Oxidation Performance of Platinum-Clad Mo-47Re Alloy

Ronald K. Clark and Terryl A. Wallace
Langley Research Center • Hampton, Virginia

National Aeronautics and Space Administration
Langley Research Center • Hampton, Virginia 23681-0001

June 1994

Acknowledgment

The authors acknowledge the support of J. S. Andrus, United Technologies, Pratt & Whitney, West Palm Beach, FL, who prepared the samples for testing and provided technical advise during conduct of the research.

Abstract

The alloy Mo-47Re has favorable mechanical properties at temperatures above 1400°C, but it undergoes severe oxidation when used in air with no protective coating. To shield the alloy from oxidation, platinum cladding has been evaluated. The unprotected alloy undergoes catastrophic oxidation under static and dynamic oxidation conditions. The platinum cladding provides good protection from static and dynamic oxidation for moderate times at 1260°C. Samples tested for longer times under static oxidation conditions experienced severe oxidation. The data suggest that oxidation results from the transport of oxygen through the grain boundaries and through the pinhole defects of the platinum cladding.

Introduction

Molybdenum-based alloys have the potential for meeting the materials requirements of many applications requiring strength values of the order of 140 MPa at temperatures as high as 1300°C. The addition of rhenium to molybdenum provides greater ductility and a lower ductile-to-brittle transition temperature than for unalloyed molybdenum (ref. 1). The solubility by percent weight of rhenium in molybdenum ranges from a maximum of 58 percent at 2500°C to 42 percent at 1000°C, and the estimated solubility at room temperature (from linear extrapolation) is 26 percent (refs. 2 and 3). The microstructure over most of the composition range is α-phase. Two intermediate phases that form in the Mo-Re system are a σ-phase and a χ-phase. The σ-phase, Mo_2Re_3 forms during thermal exposure at 1150°C and higher and reduces the ductility of the alloy. The χ-phase designated $MoRe_3$ has a limited homogeneity range.

The alloy Mo-47Re (percent weight) is one alloy from the Mo-Re system that is a candidate for use in hydrogen-fueled engines of hypersonic vehicles. Potential applications for the alloy in engines include heat exchanger tubes at temperatures up to 1260°C, combustion chamber linings at temperatures to 1370°C, and hydrogen pressures to 175 atm. The projected service life at peak temperature in such an application is about 12 hr. Because of the reactivity of molybdenum and rhenium with oxygen in air at high temperatures, some means of protecting the alloy must be devised (refs. 4 and 5). One approach to protecting the alloy is to clad it with a nonreactive impermeable barrier layer. Platinum is proposed as a candidate for use as a cladding because of its high melting point (1790°C) and chemical stability at high temperature (ref. 5).

This paper presents results from a study of the oxidation performance of Pt-clad Mo-47Re. Platinum-clad samples were tested under static and dynamic oxidation conditions at 1260°C. A single unclad sample was tested under dynamic oxidation conditions at 595°C. The static oxidation tests were conducted in an ambient pressure furnace with laboratory air. The dynamic oxidation tests were conducted in an electric arc-heated wind tunnel. Weight change, metallography, and microscopy results are presented to show the effects of oxidation on the alloy and interaction between the cladding and the alloy.

Material Samples

Samples for this study were provided by United Technologies, Pratt and Whitney, West Palm Beach, FL. The Mo-47Re alloy sheet (0.051 cm thick) used in preparing the samples was obtained from Climax Specialty Metals in a stress relieved condition. The nominal weight composition of the alloy is 47 percent rhenium and 53 percent molybdenum. Disks of the alloy were machined as follows: for use in preparing Pt-clad samples, the disks were 2.03 cm diameter by 0.051 cm thick, and for use without cladding, the disks were 2.54 cm diameter by 0.051 cm thick. The alloy disks and 0.0178-cm-thick Pt foil were wiped with a plastic scrub and washed in acetone before the cladding operation. The disks and foil were stacked so that each alloy disk was located between two Pt foil pieces. The Pt alloy sandwiches were wrapped in graphite foil and sealed under vacuum in metal cans. The graphite foil prevented bonding between the Pt foil and the metal cans. The cladding operation was achieved by hot isostatic pressure diffusion bonding of the disks between the Pt foil for 10 hr at 1094°C under vacuum (totally encapsulating the disks in Pt). The clad disks were then cut to produce disks that were 2.54 cm diameter by 0.086 cm thick.

Experiment

Two Pt-clad samples were tested under dynamic oxidation conditions at 1260°C and 666 Pa for

12.5 hr, and one Pt-clad sample was tested under static oxidation conditions in a laboratory furnace in air at 1260°C and 1 atm for 140 hr. One unclad sample was tested under dynamic oxidation conditions at 595°C and 666 Pa for about 15 min.

The dynamic oxidation tests were performed in the hypersonic materials environmental test system (HYMETS) at the Langley Research Center (ref. 6). The HYMETS is a 100-kW constrictor-arc-heated wind tunnel that uses air plus nitrogen and oxygen in ratios equivalent to air to produce the test environment. Figure 1 is a schematic diagram of the facility. Samples are mounted on stagnation model adapters attached to insertion stings so that the flow of gases is normal to sample surface. A water-cooled probe that measures the catalytic cold-wall heating rate and the surface pressure is mounted on a different insertion sting. The temperature of a sample under test is monitored with a radiometer focused on the front surface of the sample. The temperature of the sample is controlled by adjusting the power input to the arc.

Range of Test Conditions

Specimen diameter, cm	2.5
Specimen temperature, °C	800–1500
Surface pressure, Pa	400–800
Free-stream enthalpy, MJ/kg	4–11
Free-stream Mach No.	3.5–4.0
Cold-wall heating rate, kW/m^2	80–450

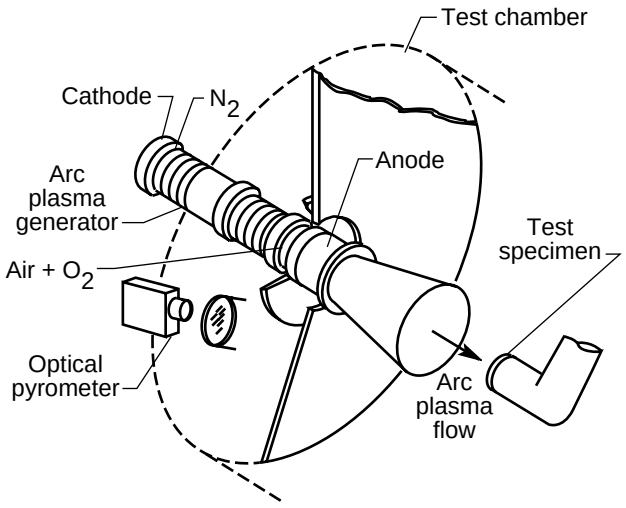

Figure 1. Schematic diagram of HYMETS facility.

The range of test conditions that can be achieved in the HYMETS are shown in figure 1. The HYMETS environment does not simulate the hydrogen-fueled engine environment. However, the HYMETS does provide high-speed flowing gas tests with oxygen, which is of critical concern to using Mo-47Re alloy in an engine application. The chemistry of the HYMETS test environment is not actively monitored. Equilibrium calculations indicate that oxygen in the test stream is almost fully dissociated (>95 percent) and nitrogen is only slightly dissociated (<5 percent) (ref. 7); however, energy balance calculations indicate that the test stream is not in equilibrium and dissociated nitrogen can be as high as 20 percent (ref. 8).

The dynamic oxidation tests consisted of 25 30-min exposure periods where each sample was exposed to the high-energy flowing air environment of the HYMETS and brought to the test temperature of 1260°C. The time required to reach the test temperature was about 100 sec. Each sample was cooled to room temperature after each 30-min exposure period to introduce a cycle effect such as would exist under service conditions.

The unclad sample was exposed to dynamic oxidation conditions for 15 min at about 595°C, which is the highest stable temperature that could be achieved. Oxidation was so severe at higher temperatures that the temperature could not be adequately controlled.

The static oxidation test of the Pt-clad sample was conducted in a laboratory furnace in air at 1260°C and 1 atm pressure. Weight change data for samples tested under static and dynamic oxidation conditions were obtained by frequently weighing the samples on an analytical balance.

Results and Discussion

Weight change data for short-time and long-time exposure of Mo-47Re are shown in figure 2. The data are based on the total surface area of the Mo-47Re disk. Figure 2(a) shows weight change data for short-time exposure of Pt-clad alloy under static and dynamic conditions. The data labeled *Dynamic* are for Pt-clad samples exposed to dynamic oxidation conditions in the HYMETS for 12.5 hr at 1260°C. The data labeled *Static* are for Pt-clad samples exposed for 140 hr in a furnace at 1260°C in laboratory air. The clad samples experienced low weight loss under static and dynamic oxidation for exposure periods up to 12.5 hr, which represents the service life for a heat exchanger of a hydrogen-fueled engine. The initial weight increase during static oxidation represents a sample weight change of about 0.2 mg and may relate to a slight buildup of stable oxides before weight loss by volatilization of oxides became important. The rate of sample weight loss is greater for dynamic oxidation than for static oxidation; however, the total

weight loss of about 1.25 mg/cm^2 after dynamic oxidation for 12.5 hr represents a material thickness change of about 100 μm, which would probably not be significant in most structural applications.

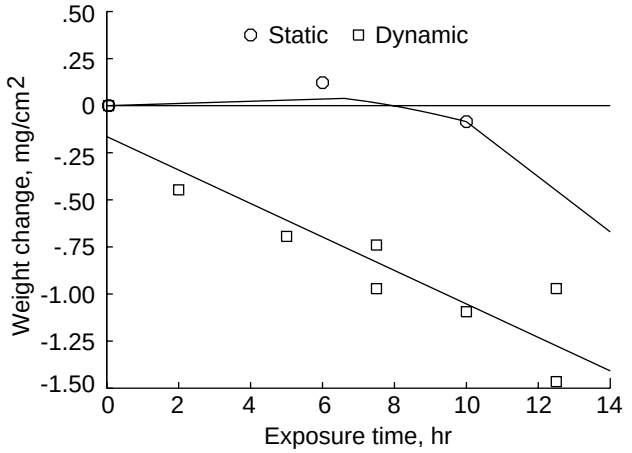

(a) Short-time oxidation data.

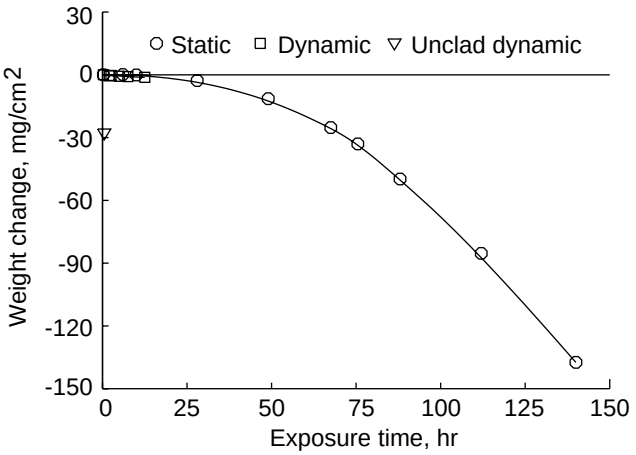

(b) Long-time oxidation data.

Figure 2. Weight change data of Pt-dad and unclad Mo-47Re samples under oxidizing condition.

The static data for longer exposure times (fig. 2(b)) show a significant weight loss with a more rapid rate of loss at times greater than 25 hr. The single data point in figure 2(b), labeled "Unclad dynamic," is for the 15-min test of a bare Mo-47Re sample in the HYMETS at 595°C. The unclad sample experienced a weight loss greater than 25 mg/cm^2 during the brief exposure to dynamic oxidation at 595°C. At temperatures above 595°C under dynamic oxidation conditions, the unclad alloy experienced rapid oxidation and the sample temperature increased uncontrollably. Because of the difficulty in controlling the temperature of the sample, this data point is judged to be qualitative only; however, it illustrates the reactivity of unprotected Mo-47Re alloy even at modest temperatures.

The weight change data for Mo-47Re can be understood by considering the oxides formed and their characteristics. When Mo-47Re alloy is heated in air, it undergoes oxidation to form MoO_2 and MoO_3 and numerous oxides of rhenium. The primary oxide formed in air, MoO_3, volatizes rapidly at temperatures above 600°C, and the primary oxide of rhenium, Re_2O_7, volatizes at 360°C (refs. 4 and 5). Thus, because of the high volatility of oxides that form, unprotected samples exposed to air at high temperature normally experience a weight loss with exposure to static or dynamic oxidation conditions.

The surface of samples were examined with a scanning electron microscope (SEM). Figure 3 shows SEM micrographs of the surface of Pt-clad samples before and after static and dynamic oxidation exposure. The surface of samples before exposure is uniformly flat with elongated markings that were imparted to the soft platinum by the graphite foil that was used to prevent adherence of the samples to the container in which they were diffusion bonded. The surfaces of the dynamic and static oxidation samples are littered with particles which energy dispersive spectroscopy (EDS) showed to be silicon rich. Possible sources of the silicon are the refractory brick of the furnace used for the static oxidation tests and a contaminant in the Pt foil (the Pt foil used for cladding was not high purity). Pinholes are identifiable along the cladding grain boundaries of the dynamic oxidation sample. The grain boundaries of the Pt cladding are also much more prominent for the static oxidation sample than for the dynamic oxidation sample. The prominence of the grain boundaries of the static oxidation sample resulted from thermal etching or thermal grooving caused by long-term high-temperature exposure of the sample (refs. 5 and 9).

Cross sections of the samples were examined with optical microscopy. Figure 4 shows micrographs of the alloy before and after exposure to static and dynamic oxidation. The substrate alloy before oxidation shows the elongated structure that resulted from rolling of the ingot to sheet. A fine second phase is distributed evenly throughout the α-phase matrix. After the thermal exposure associated with dynamic oxidation, much of the elongated structure has disappeared and the second-phase particles have increased in size. The second phase is even more prominent in the sample exposed to static oxidation. Results from wavelength dispersion spectroscopy (WDS) analysis of the two phases of the

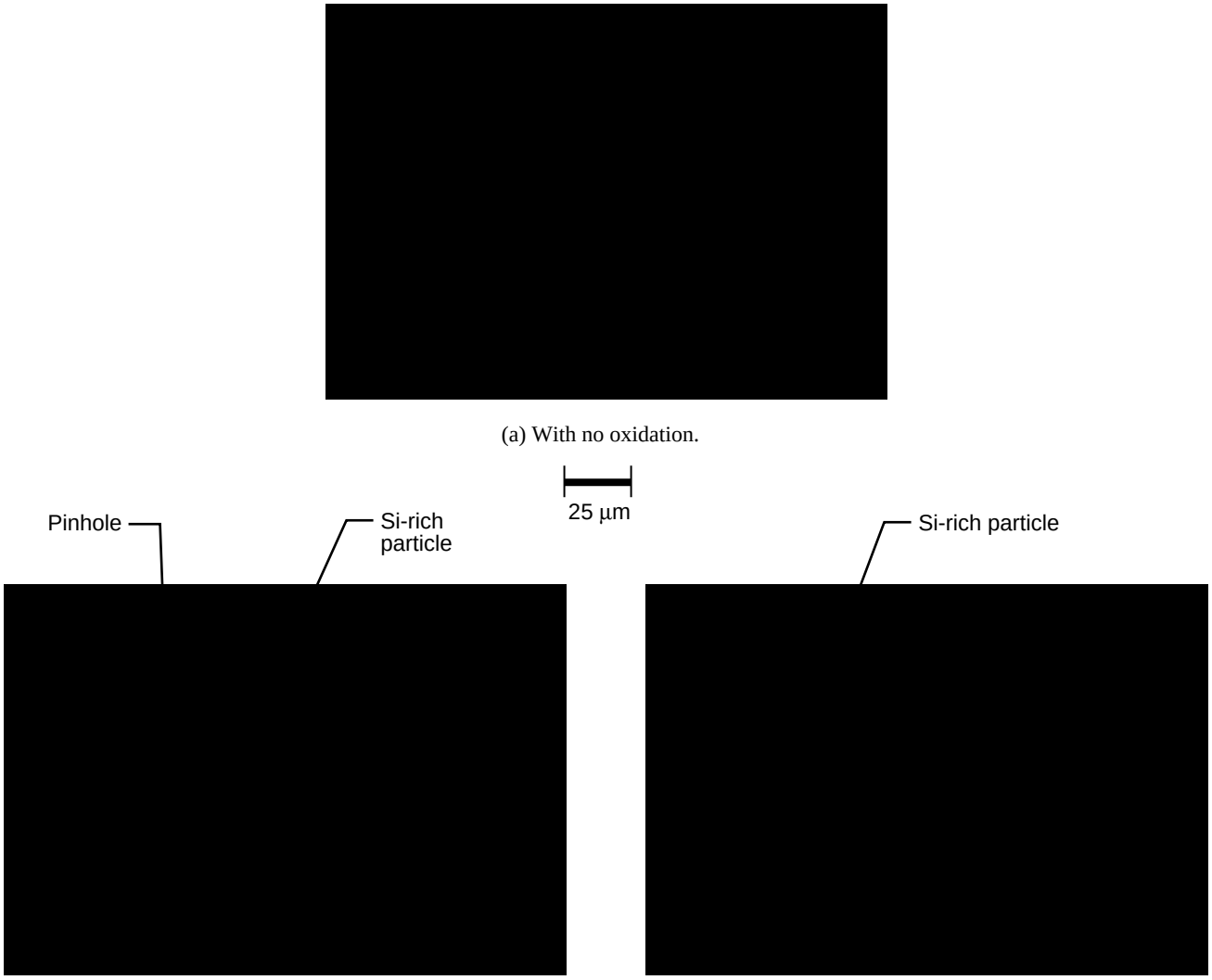

(a) With no oxidation.

(b) After dynamic oxidation for 12.5 hr.

(c) After static oxidation for 140 hr.

Figure 3. Surface of Pt-clad Mo-47Re samples before and after oxidation exposure.

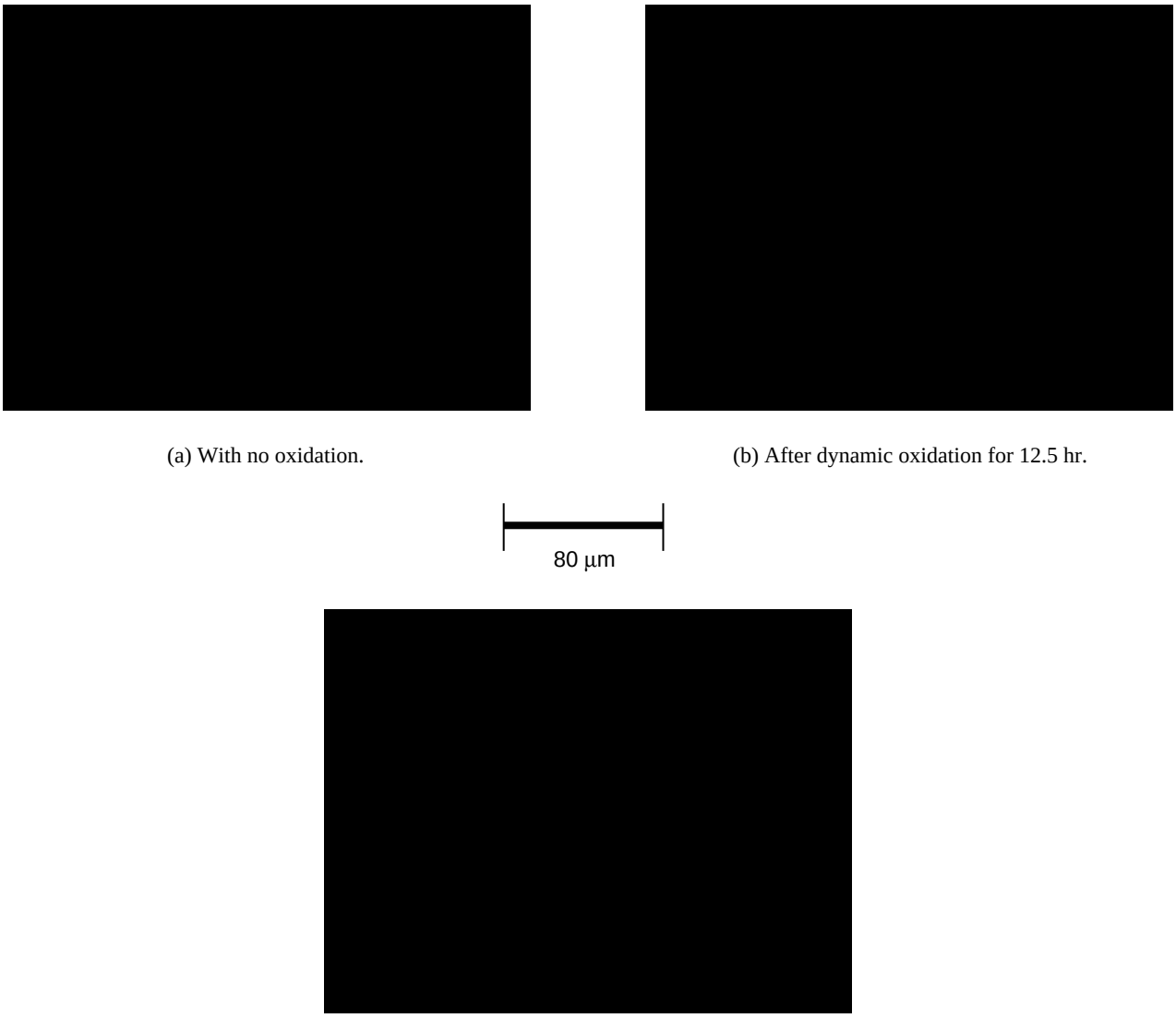

(a) With no oxidation.

(b) After dynamic oxidation for 12.5 hr.

(c) After static oxidation for 140 hr.

Figure 4. Microstructure of Mo-47Re before and after oxidation exposure.

dynamic oxidation sample are shown in table 1. The elemental composition of the second phase corresponds to that of the σ-phase (refs. 2 and 3).

Table 1. WDS Analysis of Two Phases of Pt-Clad Mo-47Re After Dynamic Oxidation for 12.5 hr at 1260°C

Element	σ-phase, percent weight	α-phase, percent weight
Mo	26.4	49.0
Re	73.6	51.0
Pt	0	0
O	0	0

Figure 5 shows optical micrographs of the reaction layer of samples before and after static and dynamic oxidation exposure. The thickness of the reaction layer changes from about 15 μm before exposure to oxidation to about 115 μm after the static oxidation exposure for 140 hr. The reaction layer of the sample exposed to dynamic oxidation is about 50 μm thick. Figure 5(b) shows clearly that the reaction layer of the sample exposed to dynamic oxidation consists of two regions of near equal thickness. The two-layer structure of the reaction layer is less obvious in the micrographs of figures 5(a) and 5(c), but this structure is easily seen under the optical microscope. Based on known thicknesses of the substrate and cladding, the boundary between the regions corresponds to the original Pt substrate interface. Table 2 shows WDS analysis results at locations indicated by the numbers in figure 5(b). Location 3 corresponds to the original Pt alloy interface. The data indicate clearly that growth of the reaction layer occurs by diffusion of molybdenum and rhenium from the alloy into the Pt cladding and by diffusion of platinum into the alloy.

Table 2. WDS Analysis at Points From Pt Cladding to Alloy Substrate

[See fig. 5 for locations]

Element	Composition, percent weight, at location—				
	1	2	3	4	5
Pt	100	79	56	39	0
Mo	0	18	21	25	50
Re	0	3	23	36	50

The optical micrographs in figure 6 show a cross-section view of samples before and after static oxidation exposure for 140 hr. In figure 6(a), the dark region at the alloy cladding interface is the thin reaction zone formed during the cladding process and is not a void. A large void does exist between the cladding and the substrate over a significant portion of the oxidized sample (fig. 6(b)). The separation of the cladding and alloy that formed the void did not occur over all regions of the sample. The interface is perfectly intact in the region toward the center of the sample. Figure 7 shows higher magnification views of the micrographs in figure 6. Figure 7(a) is typical of all areas of figure 6(a) and shows that no void exists between the alloy and the cladding. Figure 7(b) shows the region near the center of the sample after static oxidation for 140 hr (fig. 6(b)). Figure 6(b) shows that a significant loss of alloy occurred in the region of the sample edge, and figure 6(a) shows that before exposure to oxidation the Mo-47Re disk filled the region outlined by the Pt foil.

The mechanics causing separation of the cladding and alloy are not clear; however, one conjecture is that oxygen diffuses through the Pt cladding by way of grain boundaries, pinhole defects (fig. 3), and other defects in the cladding, and the oxygen then reacts with the alloy to form volatile oxides. The extensive void at the sample edge may be a result of incomplete Pt-to-Pt bonding at the edge that produced a path for oxygen to the alloy. The volatile oxides formed in the oxidation process cause an increase in pressure that causes the separation. Samples exposed to dynamic oxidation were examined by optical microscope, and there was no evidence of separation of the cladding from the alloy to form a void.

Figure 8 shows higher magnification micrographs of the sample in figure 6. These micrographs focus on a region of the substrate subjected to intense oxidation attack that has formed a large pit. The greater intensity of attack probably resulted from a pinhole defect in the Pt cladding at that point, this defect resulted in a line-of-sight region of more severe oxidation. The alloy at the point of the large pit has a band about 25 μm thick that etched differently than the remainder of the substrate. Table 3 shows results of WDS analysis of the substrate and the region of intense oxidation, which is indicated on the photomicrograph as areas A and B. The region of the pit has a high oxygen content. The severity of local attack observed here points to the potential significance of any breach of the alloy cladding in an engineering application.

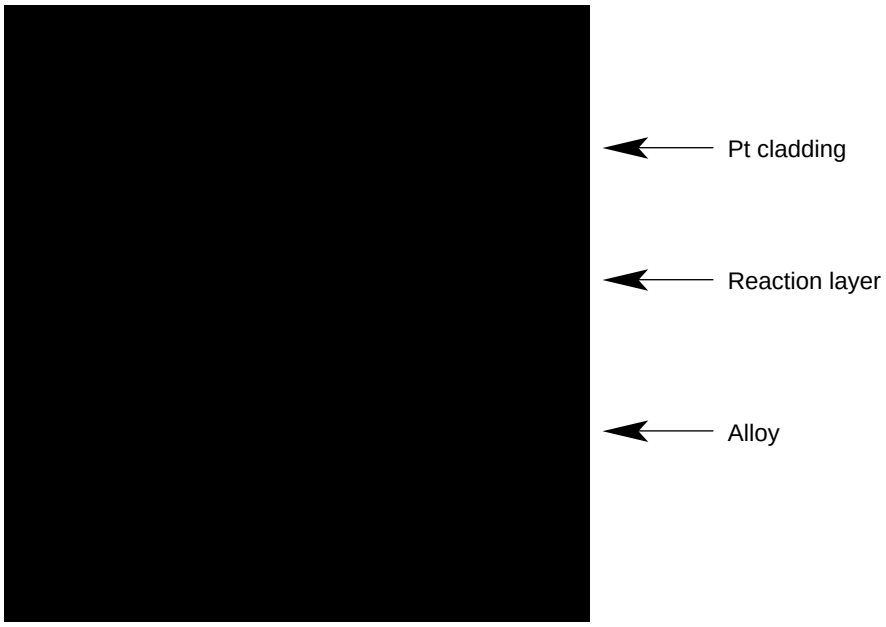

(a) With no oxidation.

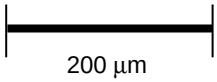

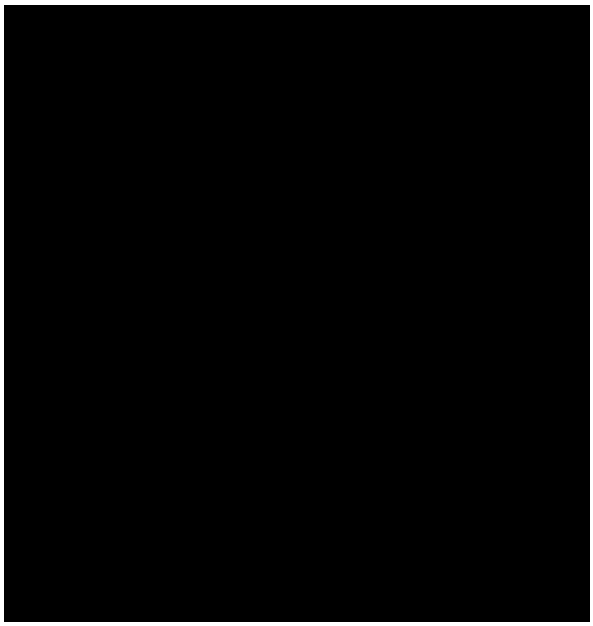

(b) After dynamic oxidation for 12.5 hr.

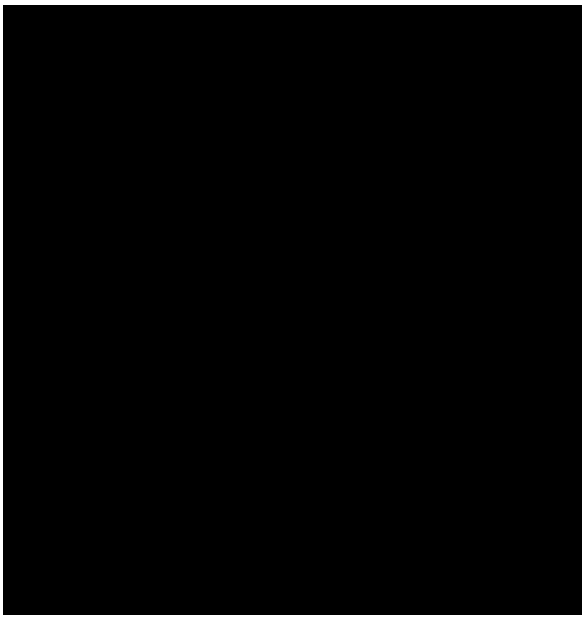

(c) After static oxidation for 140 hr.

Figure 5. Reaction layer of Pt-clad Mo-47Re samples before and after oxidation exposure.

(a) With no oxidation.

(b) After static oxidation for 140 hr.

Figure 6. Pt-clad Mo-47Re samples before and after static oxidation exposure for 140 hr.

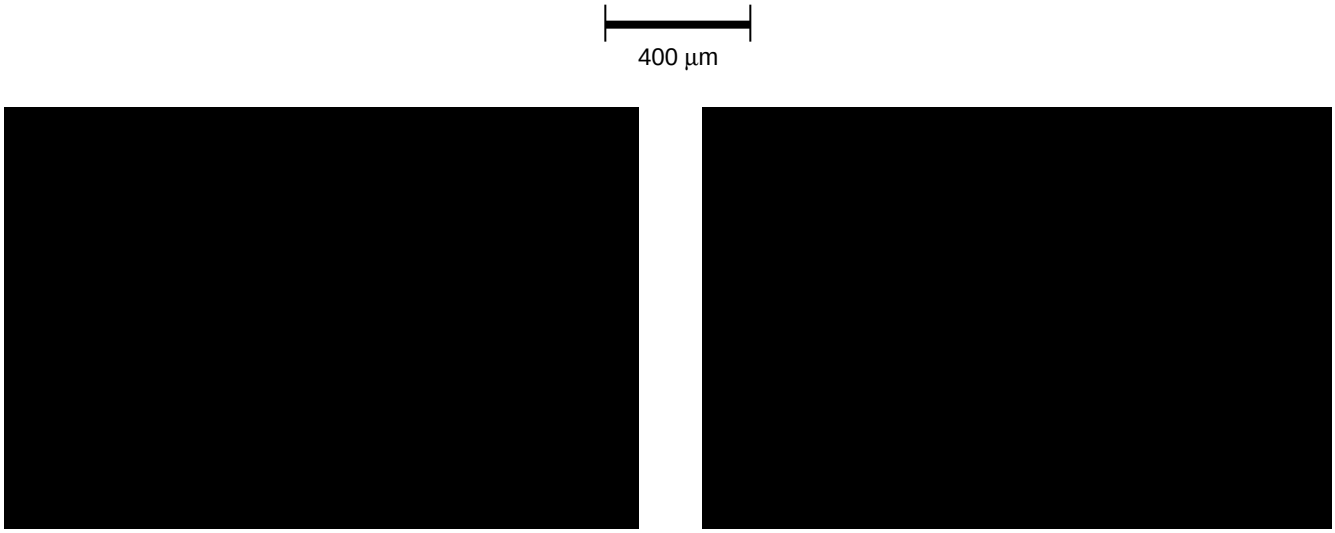

(a) Sample with no oxidation.

(b) Sample after static oxidation for 140 hr.

Figure 7. Separation of cladding from alloy of Pt-clad Mo-47Re sample after static oxidation exposure for 140 hr.

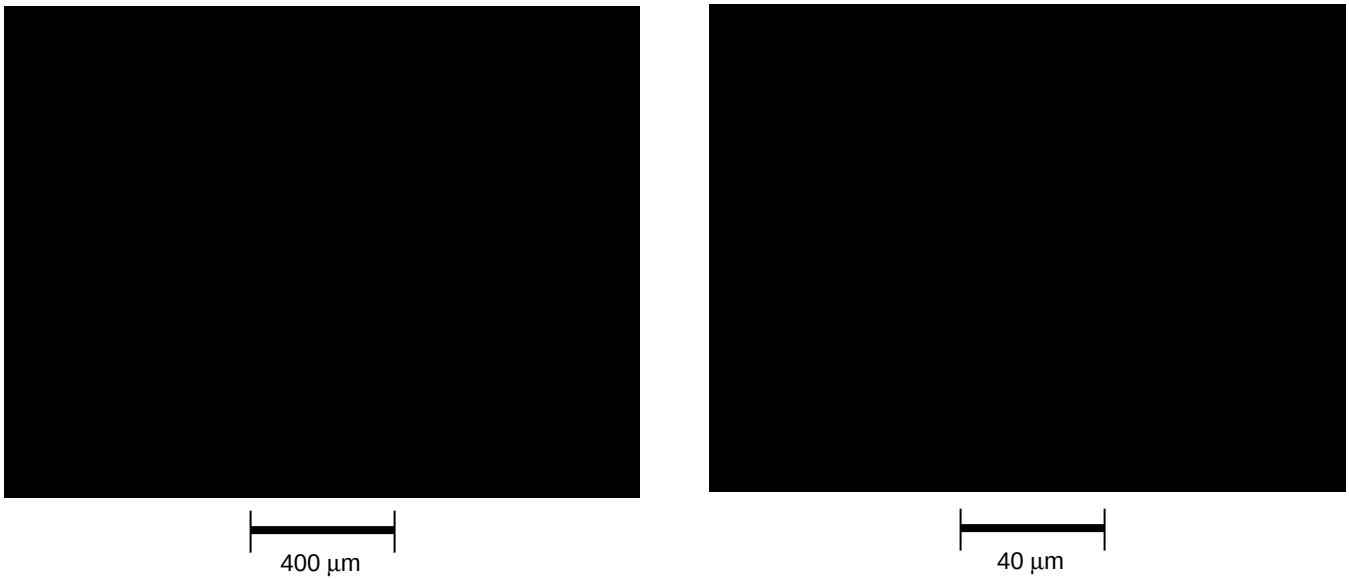

Figure 8. Details of intense oxidation attack of Pt-clad Mo-47Re sample after static oxidation exposure for 140 hr.

Table 3. WDS Analysis of Pt-Clad Mo-47Re After Static Oxidation for 140 hr at 1260°C

[See fig. 8 for location of regions]

Element	Composition, percent weight, at area—	
	A	B
Mo	59.0	51.1
Re	41.0	36.2
Pt	0	0
O	0	12.7

Concluding Remarks

Unprotected Mo-47Re alloy undergoes catastrophic oxidation when exposed to dynamic oxidation at 595°C. Platinum cladding in the form of a foil diffusion bonded to the alloy provides good protection of the alloy from oxidation during static and dynamic exposure for moderate times (about 12.5 hr) at 1260°C. The weight loss of samples exposed to dynamic oxidation is substantially greater than for samples exposed to static conditions. There is no evidence of separation of the cladding from the alloy of dynamic oxidation samples tested to 12.5 hr. Exposure of Pt-clad samples to static oxidation for longer times causes severe oxidation of the substrate and separation of the cladding from the alloy. One model for oxidation of the alloy proposes oxygen transport through grain boundaries and pinhole defects of the cladding. The alloy of samples exposed to long-time oxidation have regions of more intense oxidation resulting in large pits at the surface, ostensibly from breaches in the cladding in those areas. Thermal exposure associated with dynamic oxidation and static oxidation testing causes a large increase in the σ-phase present in the alloy.

References

1. Bryskin, Boris D.: Refractory Metals Forum: Rhenium and Its Alloys. *Adv. Mater. & Process.*, vol. 142, no. 3, Sept. 1992, pp. 22–27.
2. *Metals Handbook—8th Edition. Volume 8—Metallography, Structures and Phase Diagrams*, American Soc. Metals, 1973.
3. Elliott, Rodney P.: *Constitution of Binary Alloys, First Supplement.* McGraw-Hill Book Co., Inc., 1965.
4. Hauffe, Karl: *Oxidation of Metals.* Plenum Press, 1965.
5. *Metals Handbook—Ninth Edition. Volume 2—Properties and Selection: Nonferrous Alloys and Pure Metals*, American Soc. Metals, 1979.
6. Schaefer, John W.; Tong, Henry; Clark, Kimble J.; Suchsland, Kurt E.; and Neuner, Gary J.: *Analytic and Experimental Evaluation of Flowing Air Test Conditions for Selected Metallics in Shuttle TPS Application.* NASA CR-2531, 1975.
7. Clark, Ronald K.; Cunnington, George R., Jr.; and Robinson, John C.: Vapor-Deposited Emittance-Catalysis Coatings for Superalloys in Heat-Shield Applications. *J. Thermophys. & Heat Transf.*, vol. 1, no. 1, Jan. 1987, pp. 28–34.
8. Clark, R. K.; Cunnington, G. R.; and Wiedemann, K. E.: Experimental Evaluation of Low-Catalysis Coatings for Hypersonic Vehicle Applications. *Experimental Heat Transfer, Fluid Mechanics and Thermodynamics 1993*, Volume 2, M. D. Kelleher, K. R. Sreenivasan, R. K. Shah, and Y. Joshi, eds., Elsevire Science Publishers BV, 1993, pp. 1171–1182.
9. Reed-Hill, Robert E.: *Physical Metallurgy Principles.* Second ed., D. Van Nostrand Co., 1973.

REPORT DOCUMENTATION PAGE

Form Approved
OMB No. 0704-0188

1. AGENCY USE ONLY *(Leave blank)*	2. REPORT DATE	3. REPORT TYPE AND DATES COVERED
	June 1994	Technical Memorandum

4. TITLE AND SUBTITLE
Oxidation Performance of Platinum-Clad Mo-47Re Alloy

5. FUNDING NUMBERS
WU 763-23-41-92

6. AUTHOR(S)
Ronald K. Clark and Terryl A. Wallace

7. PERFORMING ORGANIZATION NAME(S) AND ADDRESS(ES)
NASA Langley Research Center
Hampton, VA 23681-0001

8. PERFORMING ORGANIZATION REPORT NUMBER
L-17297

9. SPONSORING/MONITORING AGENCY NAME(S) AND ADDRESS(ES)
National Aeronautics and Space Administration
Washington, DC 20546-0001

10. SPONSORING/MONITORING AGENCY REPORT NUMBER
NASA TM-4559

11. SUPPLEMENTARY NOTES

12a. DISTRIBUTION/AVAILABILITY STATEMENT
Unclassified–Unlimited

Subject Category 26

12b. DISTRIBUTION CODE

13. ABSTRACT *(Maximum 200 words)*

The alloy Mo-47Re has favorable mechanical properties at temperatures above 1400°C, but it undergoes severe oxidation when used in air with no protective coating. To shield the alloy from oxidation, platinum cladding has been evaluated. The unprotected alloy undergoes catastrophic oxidation under static and dynamic oxidation conditions. The platinum cladding provides good protection from static and dynamic oxidation for moderate times at 1260°C. Samples tested for longer times under static oxidation conditions experienced severe oxidation. The data suggest that oxidation results from the transport of oxygen through the grain boundaries and through the pinhole defects of the platinum cladding.

14. SUBJECT TERMS	15. NUMBER OF PAGES
Mo-Re alloy; Mo-47Re; Pt-clad Mo-Re; Oxidation protection through Pt cladding	11
	16. PRICE CODE: A03

17. SECURITY CLASSIFICATION OF REPORT	18. SECURITY CLASSIFICATION OF THIS PAGE	19. SECURITY CLASSIFICATION OF ABSTRACT	20. LIMITATION OF ABSTRACT
Unclassified	Unclassified		